Journal of Multidisciplinary Engineering Science and Technology (JMEST)
ISSN: 2458-9403
Vol. 5 Issue 10, October - 2018

Numerical Investigation of Separation of Air-Water Upward Flow and Experimental – CFD Flow Map and Pressure Drop Comparison

Gkoulionis A. Georgios
Mechanical Engineering and Aeronautics Dept.
University of Patras
Patras, Greece
mead6723@upnet.gr

Kokotinis G. Georgios
Mechanical Engineering and Aeronautics Dept.
University of Patras
Patras, Greece
mead6753@upnet.gr

Panopoulos A. Nikolaos
Mechanical Engineering and Aeronautics Dept.
University of Patras
Patras, Greece
panopoulos@mech.patras.gr

Margaris P. Dionissios
Mechanical Engineering and Aeronautics Dept.
University of Patras
Patras, Greece
margaris@mech.upatras.gr

Abstract*— In this study a series of numerical studies of air-water two-phase flow inside a vertical rectangular pipe are discussed. The main purpose is the investigation of partial separation of the mixture. The separator under investigation is a cavity (Plexiglas box) placed in the middle of the wide side of the pipe. The cross section of the test pipe is 25 x 55 mm and the total length is 755 mm. A series of CFD tests were carried out using Fluent 16. The flow phenomena of one constant water flow rate (33.3 L/min) with five increasing air volume rates (5, 14, 25, 36 and 53 L/min) were examined. Two cases were simulated. Initially, the separation performance was applied by applying one separator. Subsequently, the effect of applying a second separator facing the first one across the opposite side of the test pipe was investigated. The Volume of Fluid multiphase model (VOF) combined with the standard and Re-Normalisation Group (RNG) k-ε turbulence models were selected for the simulations. A flow map was designed based on theoretical calculations and experimental observations in a new a laboratory facility. Moreover, the theoretical pressure drops of multiphase flow with the homogeneous and the Friedel model were calculated.

***Keywords*— air-water flow; efficiency separation; VOF; pressure drop;**

I. INTRODUCTION

In many industrial applications, simultaneous flow of many different phases (gas, liquid, solid) is observed. The components of the mixture flow can be in the same phase, but in most of the practical applications they have different properties [1]. The two-phase flow is the simplest form of the multiphase flow. There are some different combinations of the two distinct phases, such as gas-liquid, liquid-liquid, gas-solid or liquid-solid. In this study, the gas-liquid two-phase flow (air, water) is investigated. Some parameters, which affect the distribution of the phases, are the cross section of the pipe, the mass flow rates, the orientation of the transport pipeline and the fluid properties. To simplify the description of the mixture flows, researchers designed flow map patterns [2]. Furthermore, the research sector requires reliable multiphase flow data for development and validation of fluid engineering models as well as computational fluid dynamics (CFD) codes. Most of the multiphase flow case studies, deal with experiments with water and air as working fluids. Even if this combination is not common in the practical or industrial applications the research field continues to examine the vertical air-water two-phase flow for two main reasons. The water is cheap and relatively safe as working fluid and the air can be supplied with simple equipment [3].

Several studies were carried out for investigating the two-phase flow in a vertical pipe. Azzopardi et al. (2002) studied mainly vapor-liquid flow through a Tee as a partial phase separator. They developed an approach to experimentally design a tee separator assuming the liquid flowing in a form of drops and a film in a Tee-junction before another bend. The liquid drops are assumed to pass over the junction due to their higher momentum while the gas and part of liquid film partially separate. Especially more than 90% of the gas was taken off through the tee in addition to approximately 10% of the liquid phase as the vapor, with the much lower momentum in the mixture, was easy to separate. The separation process becomes ineffective as the drop sizes get smaller. This can be concerned as a low cost and low maintenance method for vapor-liquid separation [4].

Furthermore, some studies focused on the effect of the size of pipe in the behavior of two-phase flow. Cheng at al. and Ohnuki and Akimoto show the

conventional slug flow does not occur clearly in a vertical two-phase flow for large diameter pipes. A direct transition from bubble flow to churn flow is

appeared in this case. [5, 6]. Ombere-Iyari also did not observe the traditional Taylor bubble of slug flow within the range of his work [7]. Azzopardi et al. investigated the disturbance waves in annular two-phase flow in a vertical large pipe diameter (125mm), showing that they are circumferentially localized [8]. On the other hand, Hewitt and Lovegrove observed in a small pipe diameter (32mm) a different form of waves, which appeared to be coherent around the pipe circumference [9]. Omebere-Iyari and Azzopardi, presented the time varying void fraction data and flow pattern information for the two-phase nitrogen-naphtha mixture flowing in a 189mm diameter and 52m high and compared their results for the same riser, when it was connected to an upstream horizontal pipe line of the same diameter. They found that the slug flow formed in the upstream horizontal pipe line at high liquid flowrates is propagated into the vertical pipe and is absent in the same riser when the gas and liquid phase are introduced at the riser base [10]. Except the traditional CFD software packages new techniques have been developed to solve Navier-Stokes equations when a deforming phase boundary is considerable. In marker-and-cell (MAC) method, particles are used to identify each fluid. The Volume-of-Fluid method (VOF) uses a marker function is the best example of the MAC method. The difficult application of those methods is due to the sharp boundary between the fluids and the calculation of the surface tension. Improvements on these methods have been done. For example, Scardovelli et al. [11] reviewed the VOF method, Brackbill et al. [12] developed a technique for the surface tension, Osher et al. [13] reviewed the level-set method. Other studies include the interpolation profile method (CIP) of Yabe [14] and the phase-field method of Jacqmin [15]. Johnson and Tezduyar [16] have recently produced very impressive results for the three-dimensional unsteady motion of many spherical particles. Similar studies aim to investigate a numerical method to simulate single- and multi-component fluid flows around moving/deformable solid boundaries, based on the coupling of Immersed Boundary (IB) and Lattice Boltzmann (LB) methods [17] or to present a numerical model based on the phase field and the leaky dielectric theory [18]. Boundary integral methods [19] and front-tracking methods [20] are typical explicit dynamic methods since in these methods, interfaces are treated explicitly. An advantage of explicit interface methods is that the surface tension can be accurately calculated. Phase-Field models for multi-component fluid flows have been reviewed with numerical methods [21].

In this study, a new mixture separator is proposed. It has been tested experimentally and numerically [22-25] for horizontal flow. It is characterized by operating principles governing the T-separator, gravity separators as well as centrifugal ones. Its application in vertical two-phase flow is at an early stage [26], but the first results and the flexibility of the design are promising. More analytically, the cavity separators offer some simple but important advantages. At first, the design and as well the construction method for applications is simple, cheap and can easily be adjusted in complex geometries. Secondly, there is no need for extra energy consumption to separate the mixture flow. Last but not least, the separator can be can easily be replaced and maintained. For the requirements of this investigation, a cavity separator was selected and is placed in the middle of the wide side of a vertical pipe with rectangular cross section of 25x55mm. The cavity is placed vertical to the flow direction to take advantage of the buoyancy effects and the density difference between the two phases. This separation mechanism is based on the different densities of the two phases. Especially, the air phase moves upward due to lower density while the liquid phase moves downwards due to the gravity. In horizontal two-phase flow, only the “lighter” phase is separated while in vertical two-phase flow the larger amount of the mixture that is exported from the cavity separator, consists of the “lighter” phase.

The purpose of this CFD study is to investigate the application of the cavity separator to a vertical pipe with air-water flow. Moreover, the application of one or more separators is under investigation, as well as, the flow structures that are formatted inside the tube during the separation process. The software packages for the flow visualization results of the air void fraction inside the vertical pipe, which is presented in terms of air volume fraction iso-surfaces, were the CFD commercial tool Ansys Fluent 16.0 and Ansys CFD Post [27].

II. CFD INVESTIGATION

A. Turbulence Model

The standard and RNG k-ε turbulence models were used for the Fluent simulations. The turbulence kinetic energy, k, and the dissipation rate, ε, are calculated from the following transport equations.

$$\frac{\partial}{\partial t}(\rho k)+\frac{\partial}{\partial x_i}(\rho k u_i)=\frac{\partial}{\partial x_j}(\alpha_k \mu_{eff}\frac{\partial k}{\partial x_j})+G_k+G_b-\rho\varepsilon-Y_M \quad (1)$$

The dissipation rate, ε, comes of the following equation:

$$\frac{\partial}{\partial t}(\rho \varepsilon)+\frac{\partial}{\partial x_i}(\rho \varepsilon u_i)=\frac{\partial}{\partial x_j}[(\mu+\frac{\mu_t}{\sigma_\varepsilon}]\frac{\partial \varepsilon}{\partial x_j})+C_{1\varepsilon}\frac{\varepsilon}{k}(P_k+C_{3\varepsilon}P_b)-C_{2\varepsilon}\rho\frac{\varepsilon^2}{k}+S_\varepsilon \quad (2)$$

In these equations, G_k represents the generation of turbulence kinetic energy due to the mean velocity gradients. G_b is the generation of turbulence kinetic energy due to buoyancy. Y_M represents the contribution of the fluctuating dilatation in compressible turbulence to the overall dissipation rate. The quantities α_k and α_ε are the inverse effective Prandtl numbers for k and ε, respectively. S_k and S_ε are user-defined source terms.

The RNG-based k-ε turbulence model is derived from the instantaneous Navier-Stokes equations, using a mathematical technique called ``renormalization group'' (RNG) methods. The analytical derivation results in a model with constants different from those in the standard k-ε model, and additional terms and functions in the transport equations for k and ε. A more comprehensive description of RNG theory and its application to turbulence can be found in this study [28]. The RNG model was developed using Re-Normalisation Group (RNG) methods by [29] to renormalize the Navier-Stokes equations, to account for the effects of smaller scales of motion. In the standard k-epsilon model the eddy viscosity is determined from a single turbulence length scale, so the calculated turbulent diffusion is that which occurs only at the specified scale, whereas in reality all scales of motion will contribute to the turbulent diffusion. The RNG approach, which is a mathematical technique that can be used to derive a turbulence model similar to the k-epsilon, results in a modified form of the epsilon equation which attempts to account for the different scales of motion through changes to the production term. The main difference between the RNG and standard k-ε models lies in the additional in the ε equation given by:

$$R_\varepsilon = \frac{C_\mu \rho \eta^3 \left(1-\eta/\eta_0\right)}{1+\beta\eta^3}\frac{\varepsilon^2}{k} \quad (3)$$

where η is equal to Sk/ε, η_0 is equal to 4.38 and β is equal to 0.012.

B. *Multiphase Model*

The Volume of Fluid (VOF) multiphase model is a Euler-Euler approach for multiphase flow calculation which is selected to the air-water flow regime simulation. It is designed for two-phase or more flows and is applied on a fixed Eulerian mesh. This multiphase model is appropriate to explain in detail the interface between the phases. The VOF model can record, for example, the motion of large bubbles in a liquid or the transient tracking of any liquid-gas interface. A set of n momentum equations is solved by VOF for each phase [27]. The Geo-Reconstruct scheme, the Pressure-Velocity coupling, the Coupled algorithm, are the most suitable choices for the pressure-velocity coupling methodology. The geometric reconstruction interpolation scheme is typically used whenever you are interested in the time-accurate transient behavior of the VOF solution. Enabling VOF weighting, allows the partitioning to consider the imbalance caused by the free surface reconstruction with the geo-reconstruct scheme. The Coupled allows you to apply an interface tracking method that couples the level set method with the VOF formulation. The Coupled scheme (also known as Multiphase Coupled in previous ANSYS FLUENT versions) solves all equations for phase velocity corrections and shared pressure correction simultaneously [30].

These methods incorporate the lift forces and the mass transfer terms implicitly into the general matrix. This method works very efficiently in steady state situations or for transient problems when larger time steps are required. As for the pressure, the PRESTO interpolation scheme is used, because gravity is the predominant force acting on the flow. A value of 10^{-4} is used for all residual terms except from the continuity that was set at 10^{-6} to have accurate solutions. As primary phase of the simulated flow was set water-liquid, with density ρ_w = 998.2 kg/m³ and viscosity μ_w=0.001003 kg/m·s. The secondary phase is air with properties ρ_{air} = 1.225 kg/m³ and μ_{air}=1.7894e−05 kg/m·s.

C. *Computational Domain and Grid*

In Fig. 1, the computational domain which is a pipe with rectangular cross section (25x55mm) is presented. The hydraulic diameter (D_h) for this noncircular pipe is 34mm and the cavity separator is placed in the middle of the wide side of the pipe, 350 mm (≈10 D_h) from the two-phase flow inlet. The intake of the two phases is carried out at the bottom of the pipe from different inlet surfaces. The dimensions of the cavity separator are H: 124mm, W: 55mm, Z: 55mm and as for its outlet, is circular with value Ø20mm. The total length of the pipe is 755 mm.

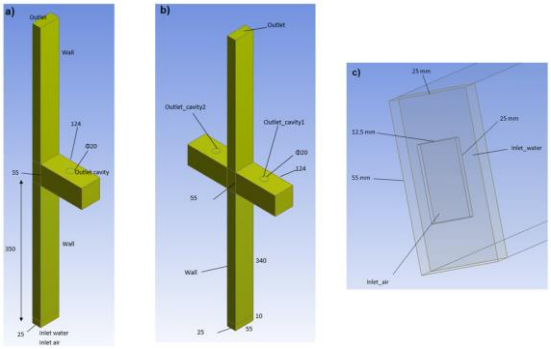

Fig. 1. *Geometry and boundary conditions (a) Case 1, (b) Case 2 (c) two phase flow inlets.*

The hydraulic diameter [31] is defined as:

$$D_h = \frac{4 \cdot A}{P} = \frac{4(a \cdot b)}{2(a+b)} = 34.375 \approx 34mm \quad (4)$$

where α: 55mm, b: 25mm, A: cross sectional area and P: the wetted perimeter of the cross-section.

The geometry is discretized with hexahedral elements (Fig. 2). The inflation method is used to generate a fine mesh near the wall.

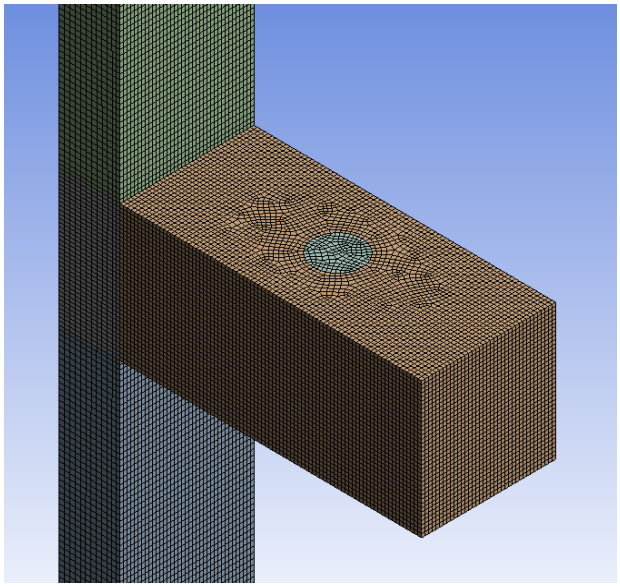

Fig. 2. *Numerical Grid (Iso plane).*

D. Grid Independence Study

It is necessary to verify a valid numerical solution which is independent of the computational grid. The air separation efficiency "n" is the parameter of interest in this simulation. The separation efficiency value "n" is defined as the ratio of the exported mean value of mass flow rate to the mean value of the total air input mass flow. Three grids were tested under the same boundary conditions to ensure that the numerical grid does not affect the solution. The three cases, that were tested, are: 256700 cells (case 1), 302000 cells (case 2) and 550000 cells (case 3). Between case 2 and case 3, the exported "n" value of the numerical solution is almost the same. A further augmentation of the grid does not differentiate the numerical value, but it increases the computational cost. For all these reasons, the grid with the 302000 cells (Fig. 2) is selected to continue to the next simulations. The air separation efficiency value "n" is a sensitive criterion to the grid density but there is no way to measure the statistical properties of air distribution in the main channel. The numerical value of "n" did not change between cases 2 and 3 and the air volume flow structures were in very good agreement with the relative experiments.

III. RESULTS

A. Flow Visualization Results

In this study only one water volume flow rate is investigated. The water volume flow rate is constant at the value of 2 m^3/h with ascending gas flow rate as presented in the following Table I:

TABLE I. BOUNDARY CONDITIONS

Q_w: 2 m^3/h	
Air velocity (m/s)	***Water velocity (m/s)***
0.27	0.52
0.75	0.52
1.33	0.52
1.92	0.52
2.83	0.52

The air-water mixture flow formation is presented in Fig. 3 and Fig. 4 and is expressed in terms of the air volume fraction. For both cases, the water superficial velocity at the inlet is equal to 0.52 m/s (2 m3/h). The air enters from the middle of the inlet and the water surround it and tends to occupy the volume towards the wall surface (Fig. 1c). In Fig. 3, the air volume fraction contour, with one cavity separator, is presented. The color scale represents the air volume fraction variable. The FLUENT software allows you to plot contour lines or profiles superimposed on the physical domain. Contour lines are lines of constant magnitude for a selected variable (isotherms, isobars, etc.). A profile plot draws these contours projected off the surface along a reference vector by an amount proportional to the value of the plotted variable at each point on the surface.

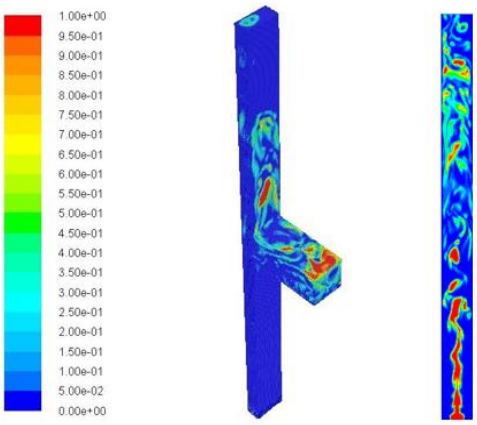

Fig. 3. *Air volume fraction - 1 cavity separator (Iso view and mid plane).*

In case 2, there are two similar cavity separators facing each other (Fig. 4). In this case, the air velocity is 1.92 m/s and the separation performance has the maximum value (n: 38%).

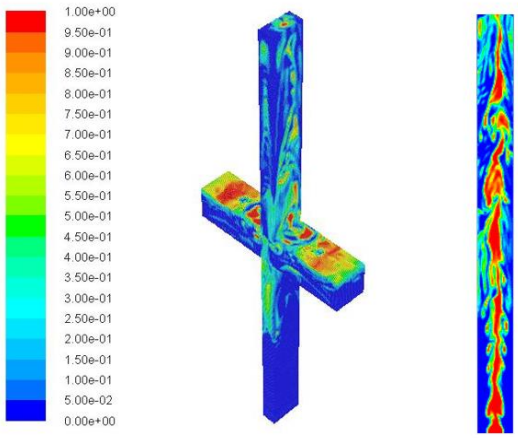

Fig. 4. *Air volume fraction - 2 cavity separators (Iso view and mid plane).*

B. Numerical Results

A "Flow rate (kg/s) – Iteration" chart (Fig. 5) was exported from Fluent for each simulation. The mass flow rate exported from the cavity outlet per iteration chart was saved. Then the average mass flow rate value is calculated to estimate the mean air separation efficiency value "n" (%). The separation efficiency value "n" is defined as the ratio of the exported mass flow rate and the total air input mass flow (5).

$$\bar{n} = \frac{\bar{Q}_{cavity}}{\bar{Q}_{inlet}} \quad (5)$$

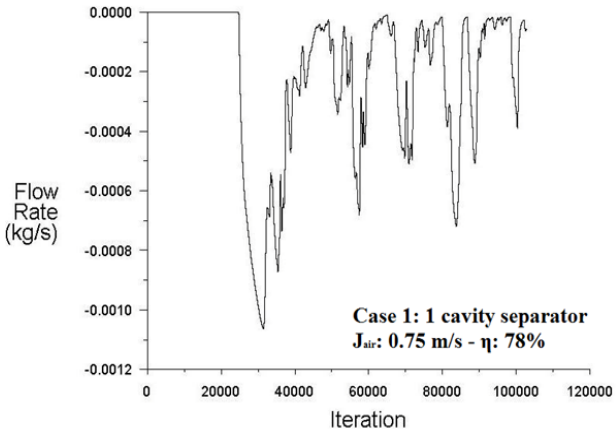

Fig. 5. *Mass Flow Rate – Iteration chart.*

The analysis to calculate the mean efficiency value is presented in Fig. 6. All the values of mass flow rate were aggregated and then we calculate the mean value by dividing with number of the values.

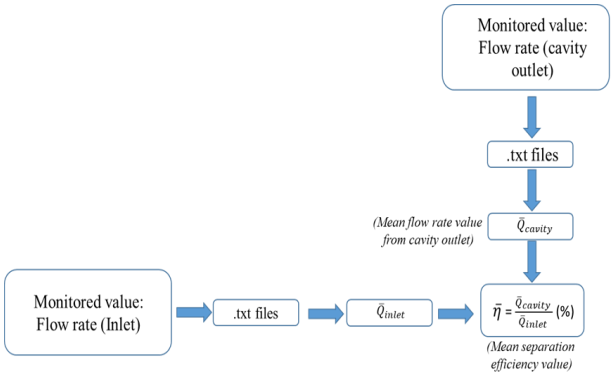

Fig. 6. *Procedure for mean separation efficiency calculation.*

The distribution of the air separation efficiency "n" as a function of the gas (air) volume flow rate (L/min) is presented in Fig. 7. The water flow rate is constant (2 m³/h) for each case. The red curve is referred to the first case, where the separation behavior of one cavity separator is investigated. It is noticed that in low air volume flow rates, the "n" values are high. The maximum value (78%) is achieved when the superficial gas velocity is 0.75 m/s. When the air volume flow rate is increased, the "n" value decreases. Concerning the second case (black curve), the separation behavior of two cavity separators is tested. In this case, the maximum "n" value is calculated when the j_{air} is 1.92 m/s and the mean value is 38%.

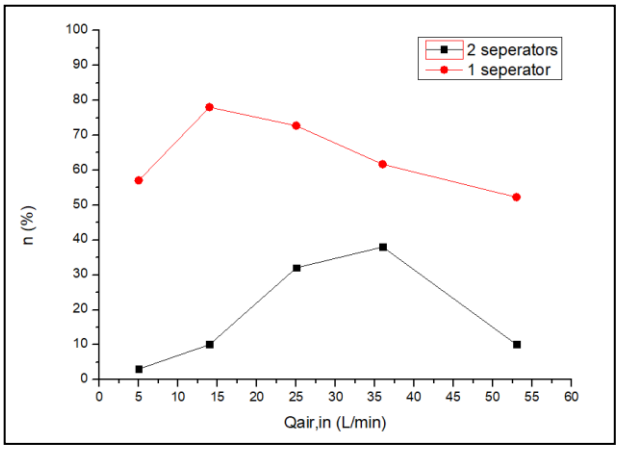

Fig. 7. *Air separation efficiency "n" - Gas (air) volume flow rate (L/min).*

The values of air separation efficiency "n" are presented in Table 2. The maximum value (78%) is achieved when the superficial gas velocity is 0.75 m/s. When the air volume flow rate is increased, the "n" value decreases. Concerning the second case (2 separators), the separation behavior of two cavity separators is tested. In this case, the maximum "n" value is calculated when the jair is 1.92 m/s and the mean value is 38%.

TABLE II. RESULTS OF AIR SEPARATION EFFICIENCY "N" USING A) ONE SEPARATOR (CASE 1) B) TWO SEPARATORS (CASE 2)

Q_{air} (L/min)	Cases	
	n (%) (Case 1)	***n (%) (Case 2)***
5	57	3
14	78	9,7
25	72,7	32,1
36	61,7	38
53	52	10

There is similar behavior on previous studies for both vertical [26] and horizontal experiments [22-25]. It is observed that there is a critical amount of mixture that can manage the separator. After this critical value the separator ignores the excessive amount of air.

IV. FLOW PATTERNS

In many industrial applications, the vertical gas-liquid flow takes place. This type of flow is considered as complex mainly because of the interaction between the liquid and the compressible phase (gas). For this reason, it is essential to find a way to describe the distribution of the two components of the mixture. This geometric distribution of the components is called flow regime or flow pattern. For different flow rates and different properties of the two phases result different flow regimes. The flow patterns of gas-liquid flow in vertical tubes described in the literature [32, 33] are presented in Fig. 8.

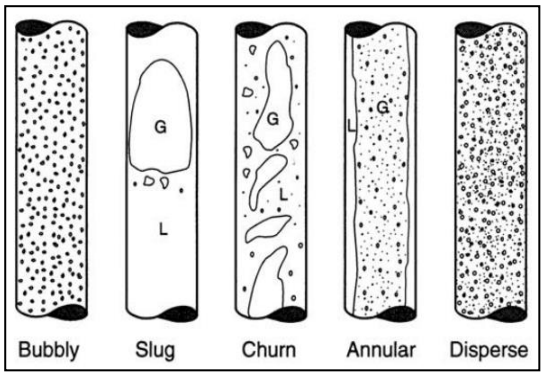

Fig. 8. *Sketches of flow regimes for two-phase flow in a vertical pipe [26].*

The CFD flow visualization tools are used to export the iso-surfaces of the air volume fraction (Fig. 9a and Fig. 9b). As the gas flow rate is increased, bubbles of air, between the liquid phases, collide and form larger bubbles. These bubbles have the shape of bullet and the flow regime is called slug. These bullet bubble's diameters are almost equal to the cross section of the pipe with a thin film of water separating them from the walls. The liquid slug area between two Taylor bubbles, as they are also called, is filled with small bubbles that are quite similar to those in bubble flow. At higher gas flow rates, because of instabilities in the slugs, churn flow is a highly disordered flow. Churn flow can be interpreted as an irregular and chaotic slug flow. However, the liquid phase is continuous and is mainly moving near the wall of the pipe. The churn flow of gas and liquid volumes is very usual in almost every cross section.

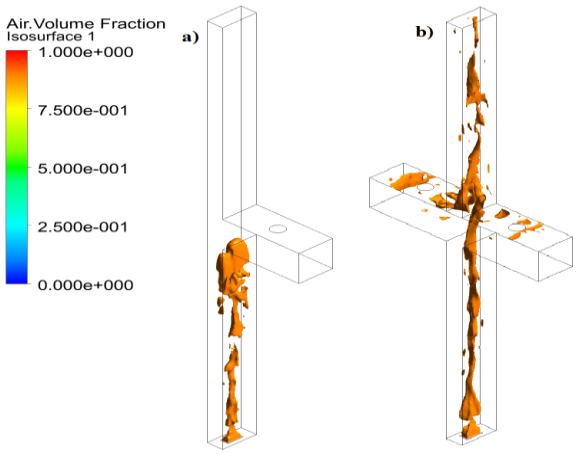

Fig. 9. *Air volume fraction iso surfaces a) Plug (Case 1), b) Churn (Case 2).*

The Hewitt & Roberts [34] flow regime map for vertical two-phase flow is presented in Fig. 10. When the air flow rate is low, the flow patter is slug. As the air superficial velocity increases the flow pattern tends to the churn bubble region. Any deviations are due to the rectangular cross-section of the duct and to the separation process.

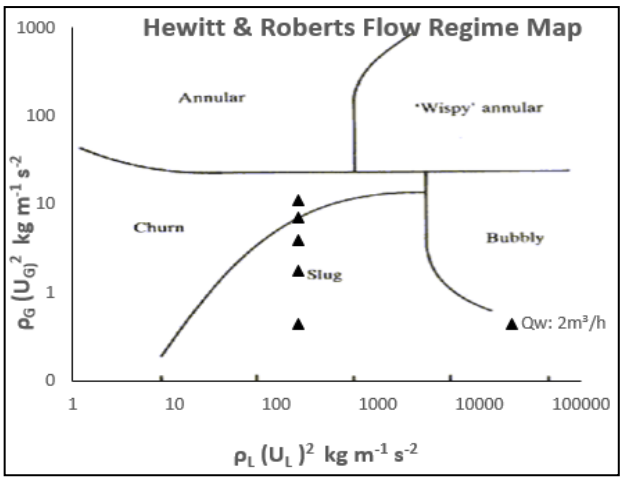

Fig. 10. *Hewitt & Roberts Flow Regime Map [27].*

The operating conditions of the churn marker for each case are:

- 1 separator: (j_w: 0.52 m/s, j_g: 0.75 m/s)
- 2 separators: (j_w: 0.52 m/s, j_g: 1.92 m/s)

The experimental flow regimes (Fig.11 a-c) and the separation process/mechanism in Fig. 11d. The theoretical calculations of the flow pattern map

indicated slug and churn flow. The validation between the flow experimental flow structures and the flow map are in very good agreement.

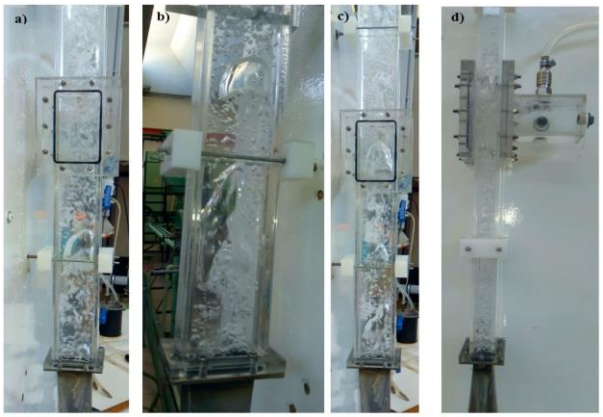

Fig.11. *Experimental flow regimes (a), (b) slug flow, (c) churn flow and (d) separation process.*

V. TWO PHASE FLOW PRESSURE DROP

In two phase flows, pressure drop depends on the flow rates of the two components and the observed flow patterns. One of the original motivations for investigating two phase flow regimes is the potential for choosing the proper flow pattern that would give the minimum pressure loss in simultaneous transport of gas and liquid in a single pipe line. A significant reduction in the pressure drop values gives the possibility of reducing the cost of pumping. The latter argument indicates the importance of prediction of pressure drop.

On this work, two models, for the calculation of pressure drop, were used. The first one, the homogeneous model considers that there is no slip velocity between the two phases. The other one, the Friedel model for two separated flows can thought more relevant to our fluent model.

A. Homogeneous Model

The total pressure drop of a fluid is due to the variation of potential energy of the fluid, kinetic energy of the fluid and that due to friction on the walls of the flow channel. Thus, the total pressure drop Δp_{total} is the sum of the static pressure drop (elevation head) Δp_{static}, the momentum pressure drop (acceleration) Δp_{mom}, and the frictional pressure drop Δp_{frict}:

$$\Delta p_{total} = \Delta p_{static} + \Delta p_{mom} + \Delta p_{frict} \quad (6)$$

The static pressure drop for a homogeneous two-phase fluid is:

$$\Delta p_{static} = \rho_H \cdot g \cdot H \cdot \sin\theta \quad (7)$$

where H is the vertical height, θ is the angle with respect to the horizontal, and the homogeneous density ρ_H is

$$\rho_H = \rho_L \cdot (1-\varepsilon_H) + \rho_G \cdot \varepsilon_H \quad (8)$$

and ρ_L and ρ_G are the liquid and gas (or vapor) densities, respectively.

The homogeneous void fraction ε_H is determined from the quality x as

$$\varepsilon_H = \frac{1}{1+\left(\frac{u_G}{u_L}\frac{(1-x)}{x}\frac{\rho_G}{\rho_L}\right)} \quad (9)$$

where u_G/u_L is the velocity ratio, or slip ratio (S), and is equal to 1.0 for a homogeneous flow. The momentum pressure gradient per unit length of the tube is:

$$\left(\frac{dp}{dz}\right)_{mom} = \frac{d\left(\frac{\dot{m}_{total}}{\rho_H}\right)}{dz} \quad (10)$$

For an adiabatic flow where x = constant, $(dp/dz)_{mom}$ is equal to zero.

The most problematic term is the frictional pressure drop, which can be expressed as a function of the two-phase friction factor f_{tp}, and for a steady flow in a channel with a constant cross-sectional area is:

$$\Delta p_{frict} = \frac{2 f_{tp} \cdot L \cdot \dot{m}_{total}^2}{d_i \cdot \rho_H} \quad (11)$$

where L is the length of the channel and d_i is its internal diameter. The friction factor may be expressed in terms of the Reynolds number by the Blasius equation:

$$f_{tp} = \frac{0.079}{\mathrm{Re}^{0.25}} \quad (12)$$

and the Reynolds number is

$$\mathrm{Re} = \frac{\dot{m}_{total} \cdot d_i}{\mu_{tp}} \quad (13)$$

The viscosity for calculating the Reynolds number can be chosen as the viscosity of the liquid phase or as a quality averaged viscosity μ_{tp}:

$$\mu_{tp} = x\mu_G + (1-x)\mu_L \quad (14)$$

The flow quality "x" [35] is defined as the ratio of the gas mass-flow rate $\dot{M}_G$ to the total mass flow rate $\dot{M}$ (in kg/s):

$$x \equiv \frac{\dot{M}_G}{\dot{M}}, \dot{M} = \dot{M}_L + \dot{M}_G \quad (15)$$

Where, $\dot{M}_L$ is the liquid mass flow rate.

B. Seperated Flow-Friedel Model

Friedel correlation is the preferred method for in tube flow when $(\mu_L/\mu_G) < 1000$ and the mass velocities less than 2000 kg/(m^2·s) [36].

The two-phase pressure drops for flows inside tubes are the sum of three contributions: the static pressure drop Δp_{static}, the momentum pressure drop Δp_{mom} and the frictional pressure drop Δp_{frict} as given by:

$$\Delta p_{total} = \Delta p_{static} + \Delta p_{mom} + \Delta p_{frict}$$

The static pressure drop is given by:

$$\Delta p_{static} = \rho_H \cdot g \cdot H \cdot \sin\theta$$

The momentum pressure drop reflects the change in kinetic energy of the flow and is for the present case given by:

$$\Delta p_{mom} = \dot{m}_{total}^2 \left\{ \left[\frac{(1-x)^2}{\rho_L(1-\varepsilon)} + \frac{x^2}{\rho_G \varepsilon} \right]_{out} - \left[\frac{(1-x)^2}{\rho_L(1-\varepsilon)} + \frac{x^2}{\rho_G \varepsilon} \right]_{in} \right\} \quad (16)$$

where $\dot{m}_{total}$ is the total mass velocity of liquid plus vapor and x is the vapor quality.

The separated flow model considers the two phases to be artificially separated into two streams, each flowing in its own pipe. The areas of the two pipes are proportional to the void fraction ε. For vertical flows, the Rouhani and Axelsson [37] expression can be used for void fractions larger than 0.1:

$$\varepsilon = \frac{x}{\rho_G} \left[\left[1 + 0.2(1-x) \left(\frac{g d_i \rho_L^2}{\dot{m}_{total}^2} \right)^{\frac{1}{4}} \right] \left(\frac{x}{\rho_G} + \frac{1-x}{\rho_L} \right) + \frac{1.18(1-x)\left[g\sigma(\rho_L - \rho_G) \right]^{0.25}}{\dot{m}_{total}^2 \rho_L^{0.5}} \right]^{-1} \quad (17)$$

The two-phase density is obtained from:

$$\rho_{tp} = \rho_L \cdot (1-\varepsilon) + \rho_G \cdot \varepsilon \quad (18)$$

The correlation method of Friedel (1979) utilizes a two-phase multiplier:

$$\Delta p_{frict} = \Delta p_L \Phi_{fr}^2 \quad (19)$$

Where, the Δp_L is calculated for the liquid-phase flow as:

$$\Delta p_L = 4 f_L \left(\frac{L}{d_i} \right) \dot{m}_{total}^2 \left(\frac{1}{2\rho_L} \right) \quad (20)$$

The liquid friction factor f_L and liquid Reynolds number (and vapor friction factor f_G and vapor Reynolds number with the vapor viscosity) are obtained from (10) and (11):

$$f_{tp} = \frac{0.079}{\mathrm{Re}^{0.25}}$$

$$\mathrm{Re} = \frac{\dot{m}_{total} \cdot d_i}{\mu_{tp}}$$

Using the liquid dynamic viscosity μ_L.

His two-phase multiplier is:

$$\Phi_{fr}^2 = \mathrm{E} + \frac{3.24FH}{Fr_H^{0.045} We_L^{0.035}} \quad (21)$$

The dimensionless factors Fr_H, E, F and H are as follows:

$$Fr_H = \frac{\dot{m}_{total}^2}{g d_i \rho_{\mathrm{H}}^2} \quad (22)$$

$$E = (1-x)^2 + x^2 \frac{\rho_L f_G}{\rho_G f_L} \quad (23)$$

$$F = x^{0.78}(1-x)^{0.224} \quad (24)$$

$$H = \left(\frac{\rho_L}{\rho_G} \right)^{0.91} \left(\frac{\mu_G}{\mu_L} \right)^{0.19} \left(1 - \frac{\mu_G}{\mu_L} \right)^{0.7} \quad (25)$$

The liquid Weber We_L is defined as:

$$We_L = \frac{\dot{m}_{total}^2 d_i}{\sigma \rho_{\mathrm{H}}} \quad (26)$$

in which Friedel used the homogeneous density ρ_H based on vapor quality:

$$\rho_H = \left(\frac{x}{\rho_G} + \frac{1-x}{\rho_L} \right)^{-1} \quad (27)$$

C. Pressure Drop Results

The pressure drops results which is the sum of the friction pressure drop, the momentum and the static pressure drop are presented on Table III. The Friedel model does calculates almost constant pressure drop and the homogenous model has different behavior. It decreases with the increase of the air supply. The above observations are presented in Fig. 12.

TABLE III. RESULTS OF PRESSURE DROP USING HOMOGENEOUS MODEL, SEPARATED MODEL OF FRIEDEL AND FLUENT ΔP RESULTS.

Q_{air} (L/min)	Q_w: 2 m³/h			
	Homo-geneous Model ΔP (kPa)	***Friedel Model ΔP (kPa)***	***One separator ΔP (kPa)***	***Two separators ΔP (kPa)***
5	6.91	8.25	6.80	5.60
14	5.60	8.19	6.60	5.10
25	4.55	8.15	6.42	5.00
36	3.83	8.12	6.45	3.80
53	3.08	8.09	4.05	3.6

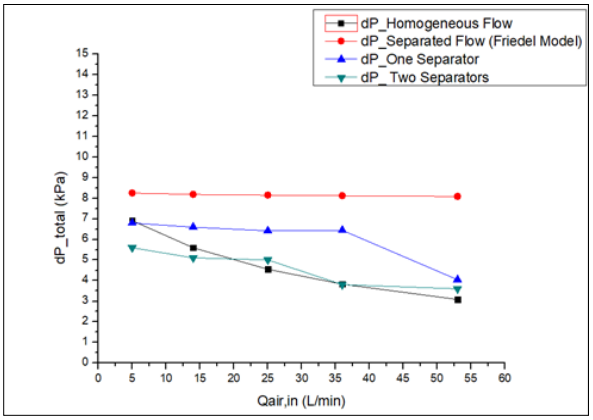

Fig. 12. *Comparison of pressure drop models.*

The homogeneous model is the simplest approach for the analysis of two–phase mixture flow (gas-liquid) inside pipes. This model can generally give reasonable results for high pressures and high mass fluxes. However, it should be preferred for practical applications, one of the separated flow models. All the separated models for the prediction of pressure drop are based on Homogeneous Model.

VI. CONCLUSION

The separation performance of a new kind of mixture separator, called cavity separator, is investigated numerically in this study using the commercial CFD tool Ansys Fluent. The simulations were performed within a flow domain of 755mm long with one (case 1) or two (case 2) cavity separators fitted at $10D_h$ from the inlet (D_h: 34mm hydraulic diameter) with air and water as working fluids. The comparison of the air separation efficiency results between the two cases based on time series of void fraction lead to the following conclusions:

Case 1

- The best separation efficiency is 78% (j_{air}: 0.75 m/s).
- Slug flow pattern.
- Range of numerical efficiency values: 52%<n<78%.
- All the case 1 efficiency values are higher than ones of case 2 ($n_{s1}<n_{s2}$).
- Range of numerical efficiency values: 52%<n<78%.
- All the case 1 efficiency values are higher than the ones of case 2 ($n_{s1}>n_{s2}$).

Case 2

- Slug and churn flow pattern.
- Range of numerical efficiency values: 3%<n<38%.
- When two cavity separators are used, large air bubbles are trapped inside the cavities and cannot escape through the cavity outlet or recirculate inside the cavity (Fig. 4).

The experimental flow patterns (slug and churn) are validated with the experimental ones (Fig. 8-10) with very good agreement.

ACKNOWLEDGMENT

The present work was financially supported by the «Andreas Mentzelopoulos Scholarships University of Patras».

REFERENCES

[1] M.B. Swanand, “Study of Flow Patterns and Void Fraction in Vertical Downward Two-Phase Flow,” Bachelor, Dept. Mech. Eng., Amravati Univ., Amravati, MA, 2011.

[2] S. Sharaf, Peter van der Meulen, O. E. Agunlejika and B. Azzopardi, “Structures in gas-liquid churn flow in a large diameter vertical pipe, International Journal of Multiphase Flow,” vol. 78, no. 1, pp. 88-103, 2016.

[3] L. Szalinski, L.A. Abdulkareem, M.J. Da Silva, S. Thiele, M. Beyer and D. Lucas, “Flow characteristics of refrigerant and oil mixture in an oil separator,” International Chemical Engineering Science, vol. 65, No. 1, pp. 3836-3848, 2010.

[4] B.J. Azzopardi, D.A. Colman and D. Nicholson, “Plant application of a T-junction as a partial phase separator,” Institution of Chemical Engineers Trans IChemE Part A, vol. 80, no. 1, pp. 87-96, 2002.

[5] H. Cheng, J.H. Hills and B. J. Azzopardi, “A study of the bubble to slug transition in vertical gas liquid flow in columns of different diameters,” International Journal of Multiphase Flow, vol. 24, no. 1, pp. 431-452, 1998.

[6] A. Ohnuki and H. Akimoto, “Experimental study on transition of flow pattern and phase distribution in upward air water two phase flow along a large vertical pipe,” International Journal of Multiphase Flow, vol. 26, no. 1, pp. 367-386, 2000.

[7] N.K. Ombebe-Iyari, “The effect of pipe diameter and pressure in vertical two-phase flow,” Ph.D. Thesis, Dept. Environmental and Mining Eng., Nottingham Univ., Nottingham, MA, 2006.

[8] B.J. Azzopardi, S. Taylor and D.B. Gibbons, “Annular two-phase flow in a large diameter tube,” Proc. Int. Conf. Physical Modelling of Multi-phase Flow, Coventry, 1983, pp. 267–282.

[9] G.F. Hewitt and P.C. Lovegrove, “Frequency and velocity measurements of disturbance waves in annular two-phase flow,” UKAEA Report AERE R4304, 1969.

[10] N.K. Omebere-Iyari and B.J. Azzopardi, “Gas/liquid flow in a large riser: effect of upstream configurations,” Proc. 13th Int. Conf. on Multiphase Production Technology ´07, Edinburgh, 2007

[11] R. Scardovelli and S. Zaleski, “Direct numerical simulation of free-surface and interfacial flow,” Annual Review of Fluid Mechanics, vol. 31, no. 1, pp. 567-603, 1999.

[12] J.U. Brackbill, D.B. Kothe and C. Zemach, “A continuum method for modeling surface tension,” Journal of Computational Physics, vol. 100, no. 1, pp. 335, 1992.

[13] S. Osher and R.P. Fedkiw, “Level set methods: An overview and some results,” Journal of Computational Physics, vol. 169, no. 1, pp. 463, 2001.

[14] T. Yabe, “Interface capturing and universal solution of solid, liquid and gas by CIP method,” Proc. of the High-Performance Computing of Multiphase Flow, Tokyo, 1997

[15] D. Jacqmin, "Calculation of two-phase Navier-Stokes flows using phase-field modeling," Journal of Computational Physics, vol. 155, no. 1, pp. 96, 1999.

[16] A.A. Johnson and T.E. Tezduyar, "3D simulation of fluid-particle interactions with the number of particles reaching 100," Computed Methods in Applied Mechanics and Engineering, vol. 145, no. 1, pp. 301, 1997.

[17] Z. Li, J. Favier, U. D'Ortona and S. Poncet, "An immersed boundary-lattice Boltzmann method for single- and multi-component fluid flows," Journal of Computational Physics, vol. 304, no. 1, pp. 424-440, 2016.

[18] Y. Lin, P. Skjetne and A. Carlson, "A phase field model for multiphase electro-hydrodynamic flow," International Journal of Multiphase Flow, vol. 45, no. 1, pp. 1-11, 20112.

[19] J.D. Sherwood, "Breakup of fluid droplets in electric and magnetic fields," Journal of Fluid Mechanics, vol. 188, no. 1, pp. 113-146, 1988.

[20] S.O. Unverdi and G. Tryggvason, "An immersed boundary-lattice Boltzmann method for single- and multi-component fluid flows," Journal of Computational Physics, vol. 100, no. 1, pp. 25-37, 1992.

[21] J. Kim, "Phase-Field Models for Multi-Component Fluid Flows," Communications in Computational Physics, vol. 12, n. 3, pp. 613-661, 2012.

[22] N.A. Panopoulos, D.P. Margaris and A.K. Andriopoulos, "Air separation investigation of gas-liquid stratified - slug flow along horizontal pipe: simulation and experiment," Proc. 7th Int. Conf. from Scientific Computing to Computational Engineering, Athens, 2016

[23] N.A. Panopoulos and D. P. Margaris, "Numerical Analysis of air-water separation in orthogonal pipe with parametrical outlet position," Proc. 10th Greek National Conf. Fluid Flow Phenomena, Patras, 2016

[24] N.A. Panopoulos and D.P. Margaris, "CFD simulation of street canyon phenomenon as gas-liquid two-phase flow separation mechanism," Proc. 6th Int. Conf. from Scientific Computing to Computational Engineering, Athens, 2014

[25] N.A. Panopoulos and D.P. Margaris, "Computational study of pipe with street canyon cavities as an air-water mixture pathetic separator," Proc. 9th Greek National Conf. Fluid Flow Phenomena, Athens, 2014

[26] N.A. Panopoulos and D.P. Margaris, "CFD investigation of air-water separation using a cavity separator in vertical slug and churn flow," Journal of Multidisciplinary Science and Technology (JMEST), vol. 4, no. 1, pp. 6482-6487, 2017. (Issue 1)

[27] ANSYS Inc. ANSYS Fluent User's Guide, Release 15, 2013.

[28] D. Choudhury, "Introduction to the Renormalization Group Method and Turbulence Modeling," Fluent Inc. Technical Memorandum TM-107, 1993.

[29] V. Yakhot, S.A. Orszag, S. Thangam, T.B. Gatski and C.G. Speziale, "Development of turbulence models for shear flows by a double expansion technique," Physics of Fluids A, vol. 4, no. 7, pp. 1510-1520, 1992.

[30] A. Chobadian and S.A. Vasquez, "A General Purpose Implicit Coupled Algorithm for the Solution of Eulerian Multiphase Transport Equation," Proc. Int. Conf. on Multiphase Flow, Leipzig, 2007

[31] G. Hestroni, In McGraw-Hill (Ed.), Handbook of Multiphase systems, 4 (New York-Washington: Hemisphere Pub. Corp., 1982, 154-196).

[32] T.R. John, "Two-Phase Pressure Drop inside Tubes," Chapter 13, Laboratory of Heat and Mass Transfer, Swiss Federal Institute of Technology Lausanne, Switzerland (accessed on 15/12/2017).

[33] J. Weisman, "Two-Phase Flow Patterns," In N.P. Cheremisinoff, R. Gupta, 2nd edition (Ed.), Handbook of Fluids in Motion, 4 (: Ann Arbor Science Pub., 1983, 409-425).

[34] P. B. Whalley, Boiling, condensation, and gas-liquid flow. Oxford Oxfordshire. New York: Clarendon Press; Oxford University Press, 1987. xi, 291.

[35] Jacopo Buongiorno, NOTES ON TWO-PHASE FLOW, BOILING HEAT TRANSFER, AND BOILING CRISES IN PWRs AND BWRs, MIT Department of Nuclear Science and Engineering, https://ocw.mit.edu/courses/nuclear-engineering/22-06-engineering-of-nuclear-systems-fall-2010/lectures-and-readings/MIT22_06F10_lec13.pdf (accessed on 16/01/2017).

[36] L. Friedel, "Improved friction pressure drop correlations for horizontal and vertical two-phase flow," 3R Int., 18 (7) (1979), pp. 485-491

[37] S. Z. Rouhani and E. Axelsson, "Calculation of void fraction in the subcooled and quality boiling regions," International Journal of Heat and Mass Transfer, vol. 13, no. 2, pp. 383-393, 1970. (issue2)